BILINGUAL PUBLISHING GROUP

Journal of Environmental & Earth Sciences

https://journals.bilpubgroup.com/index.php/jees

ARTICLE

Volcanic Geomorphology and Morphometry Classification of Cinder Cone in Harrat Lunayyir Saudi Arabia by Using GIS and Remote Sensing

Azizah Aziz al Shehri

Department of Geography, Imam Muhammad Ibn Saud Islamic University, Riyadh 11432, Saudi Arabia

ABSTRACT

Harrat Lunayyir, a volcanic field in western Saudi Arabia, exhibits diverse geomorphological and topographical features shaped by volcanic, tectonic, and climatic processes. This study integrates field observations, remote sensing, and GIS analysis to investigate the spatial distribution and relationships between volcanic landforms, lava flows, and topographical variation result obtained is a morphological classification of the cinder cones of Harrat Lunayyir, which can be sub-divided into four types: tephra rings, horseshoe-shaped volcanoes, multiple volcanoes and volcanoes without craters.All of these are monogenetic volcanoes, unlike central volcanoes (stratovolcanoes) which live for tens or hundreds of thousands of years and erupt numerous times. In Harrat Lunayyir, there is a clear dominance of arched horseshoe-shaped volcanoes (58) over ring-shaped cinder cones (10), A1_symmetric cones (circular, uniform cinder cones with a single crater) (32), A2_asymmetric cones (elongated, irregular cones and may feature one or more craters) (8), volcanoes without craters (55) and multiple volcanoes (20). The classification presented in this paper makes it possible to include all morphological types of volcanoes found in the region. This fact also renders the present classification a useful tool to apply in other, both insular and continental volcanic areas to eventually analyze and systematize the study of eruptive edifices with similar traits. Hence, this research will explore the standard physical volcanology literature so as to follow accepted definitions.

Keywords: GIS; Morphology; DEM; Topography; Lithology; Cinder Cones

*CORRESPONDING AUTHOR:

Azizah Aziz al Shehri, Department of Geography, Imam Muhammad Ibn Saud Islamic University, Riyadh 11432, Saudi Arabia;
Email: azizahzz@yahoo.com

ARTICLE INFO

Received: 24 February 2025 | Revised: 25 March 2025 | Accepted: 1 April 2025 | Published Online: 8 May 2025
DOI: https://doi.org/10.30564/jees.v7i5.8859

CITATION

al Shehri, A.A., 2025. Volcanic Geomorphology and Morphometry Classification of Cinder Cone in Harrat Lunayyir Saudi Arabia by Using GIS and Remote Sensing. Journal of Environmental & Earth Sciences. 7(5): 304–318. DOI: https://doi.org/10.30564/jees.v7i5.8859

1. Introduction

Volcanic processes are inherently intricate and varied, leading to significant differences in land features, deposits, along with profound impacts on the nearby surroundings [1]. In recent years, particularly post-2010, a diverse range of research has focused on the morphological aspects of land formations. The growing emphasis on this subject was triggered by the eruption of the St. Helens volcano in 1980, prompting researchers to explore interpretations of extraterrestrial shapes. The 1980 eruption of Mount St. Helens drastically altered the landscape by producing complex landforms. Similar factors are observed on extraterrestrial bodies, such as Mars and the Moon. Based on this evidence, the event spurred researchers to study volcanic geomorphology in greater detail through its comparisons between terrestrial and extraterrestrial volcanic processes. In this context of the study, it is relevant and contextual that the eruption's morphological impact provided valuable analogs for interpreting planetary surfaces through crater formation and lava flows by advancing remote sensing and GIS applications in geomorphological studies [2].

Pyroclastic cinder cones are recognized as the most basic and widespread type of continental volcanic formations on the planet. They frequently create extensive cinder-cone fields, covering hundreds of square kilometres with a few to hundreds of cones, sometimes in conjunction with polygenetic shield volcanoes [3]. An uncommon trait found in cinder cones is their well-defined initial formation dates. Often referred to as scoria cones, they have a conical structure composed of fragments explosively ejected and are capped by a bowl-shaped crater. Cinder cones are built from loose pyroclastic fragments, whereas spatter cones form from lava clots that partially fuse upon landing. These cones are commonly found in extensive fields, consisting of dozens to hundreds of cones, often associated with polygenetic shield volcanoes. Another discernible characteristic is their prolonged duration, lasting up to several million years. Individual cinder cones typically form in a single eruption where volcanic fields remain active for hundreds of thousands to millions of years due to continued eruptions at different sites. For instance, Martian volcanic fields can persist much longer than Earth's, as volcanic activity on Mars is not influenced by plate tectonics. These petite volcanoes typically share similarities in structure and composition and are grouped together in clusters within volcanic fields or on the slopes of larger polygenetic (central) volcanoes.

The shape of cinder cones is conical where they form from fragments explosively by the eruptions at their summit. On the other hand, scoria cones usually occur in distinct fields on flat surfaces by clustering in volcanic fields on the slopes of larger volcanoes. However, their formation contrasts with spatter cones through the deposition of fused lava clots and tephra rings, lava rings, explosive craters, pseudocraters, and pit craters. The distribution and arrangement of scoria cones reflect the interplay between regional tectonics and monogenetic eruption patterns [4].

Moreover, similar patterns have been observed in the Michoacán-Guanajuato volcanic field in Mexico, where craterless cones have been linked to lava ponding through secondary eruptions within the main edifice. Future studies should integrate remote sensing techniques with "InSAR (Interferometric Synthetic Aperture Radar)" to monitor surface deformation and detect active magma movement [5]. Additionally, a multidisciplinary approach has incorporated rock dating methods such as Ar-Ar geochronology, which would help establish precise eruption timelines.

This context discussion has highlighted the significance of morphometric classification in understanding the geological evolution of Harrat Lunayyir. It emphasizes the role of tectonic activity and magma dynamics which can be compared with previous studies through demonstrating both similarities and unique aspects of the volcanic field [6]. The methodology has been associated with this study where it could be enhanced with additional geochemical and geophysical data. The classification of volcanic structures has broad applications from hazard assessment to planetary geology by underscoring the need for continued research in this region.

2. Geological and Geomorphological Setting of Harrat Lunayyir

The separation between the Africa and the Arabian plates through the Red Sea and the Gulf of Aden rifts 10–15 Ma before Arabia started its approach toward Eurasia [3]. The Arabian Plate represents a geologic entity that physically moves away from Africa, contributing to the formation of the Red Sea. The Spanish Plate lies to the north of the Harrat Lunayyir, while the Anatolian Plate is located to the north,

and the Eurasian Plate to the east. Scientific opinions support that the Arabian Plate established itself through the African Rift tectonic activities. At 30 million years ago the tectonic events that formed the Red Sea began as Afar started its rifting process while sinister strike–slip movements along the Gulf of Aqaba–Dead Sea transform fault system took place. The rift process extended both in eastern and northern directions to create the Gulf of Aden and the Red Sea, respectively. The widespread acceptance now recognizes the late Oligocene (28–24 Ma) as the moment when the Red Sea rift basins first formed (**Figure 1**).

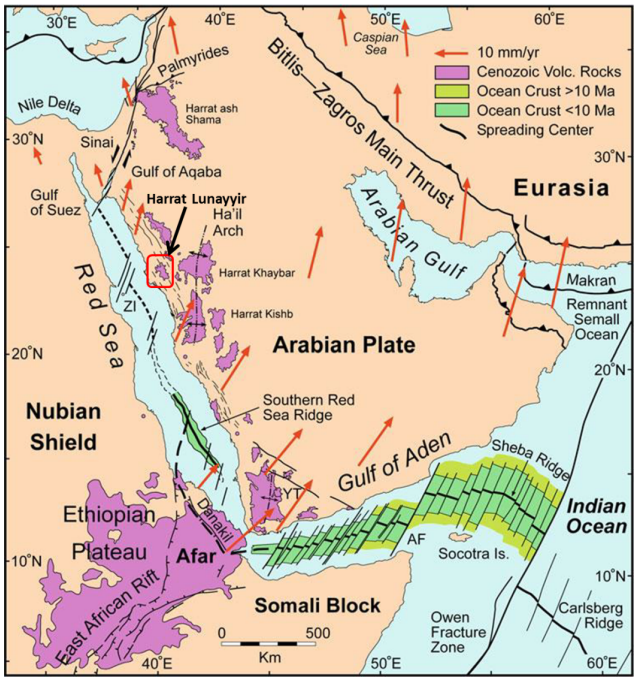

Figure 1. Tectonic map of the Red Sea rift system, including the Ethiopian (East African) rift, Afar and Gulfs of Aden, Aqaba and Suez.

Rifting of the Precambrian continental lithosphere started in the late Oligocene as the Red Sea system began separating from the Precambrian continental lithosphere before spreading throughout the seafloor. The current rift process led to Red Sea basin expansion by spreading from north to south. Presently, the Red Sea stretches through geologic positions from 30° N which marks the northern Gulf of Suez boundaries down to 12.5° N where it unites with the Gulf of Aden. The north–south stretch of the Red Sea amounts to approximately 2,250 kilometers while its maximum east–west dimension reaches 354 kilometers. The oceanic crust extends into two zones with maximum dimensions totaling approximately 100 kilometers. Seafloor spreading shows the preliminary development of oceans based on the Red Sea perspective[7]. The rift system extends across an entire continental scale from the Dead Sea to Mozambique. Geologists applying the 'Afro-Arabian rift system' terminology to its divided zones has grown in popularity through studies of this system. The expanding of the Red Sea formed Harrat Lunayyir through volcanic field development and the extension of the Arabian Shield along with associated dyke swarms.

One-third of the Arabian Peninsula consists of the Arabian Shield. Its estimated area is 670,000–725,000 km^2. A total estimated area of 2.7 × 106 km^2 encompasses the larger group called the Arabian–Nubian Shield that includes the Arabian Shield. At Harrat Lunayyir, the Arabian plate reveals its upper crustal composition which includes a crystalline Precambrian basement together with Phanerozoic sedimentary cover and Cenozoic flood basalt (**Figure 2**)[8]. The northeastern portion of the Red Sea reveals the exposed highlands of Yemen and the central Saudi Arabian region known as Najd. The western Arabian shield has geological and topographic characteristics that separate it from the eastern platform configuration. The shield surface includes plutonic rocks which make up half of the total areas and volcanic and sedimentary rock areas account for the remaining half (The platform is covered by as much as 10 km Phanerozoic sediment)[9]. Research shows that the platform crust achieved stability during the time period between ~700 Ma and approximately 150 Ma. The shield reached stability approximately 150 million years after it finished undergoing multiple periods of metamorphism and tectonic and plutonic activity.

The Arabian Shield exhibits a typical crustal measurement of 40 kilometers deep although near Red Sea coastline this figure drops to 23 to 25 kilometers deep. A 25–26 km crust layer exists throughout the western coastal Nubian Shield in Egypt between 50 km from the Red Sea shores. The Nubian Shield also displays this similar crustal characteristic as it extends into the western portion of the Red Sea. On the Egyptian coast of the Red Sea the crust extends 25–26 km thick for 50 km outwards from the shore.

The younger harrats together with transitional-to-strongly-alkalic lavas have been progressively forming along the Makkah-Madinah-Nafud (MMN) volcanic line since 12 million years. Approximately 50 monogenetic craters of variously sized volcanic cones contributed to the formulation of this region[10]. The basaltic lava flows can be characterised

by two specific segments: The first is the Tertiary unit, the Jarad basalt, which is considerably older, and the second is the Quaternary unit, the Maqrah basalt, which is younger (**Figure 3**).

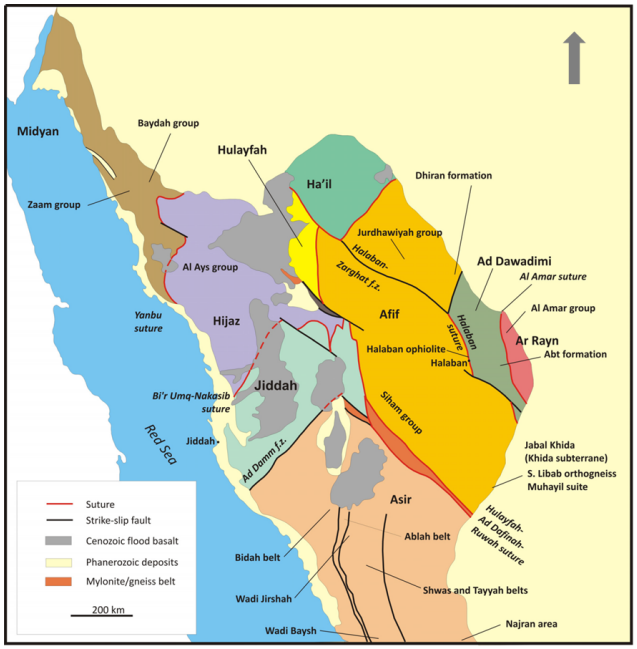

Figure 2. Lithostratigraphic units and terrane boundaries in the Arabian shield, Saudi Arabia.

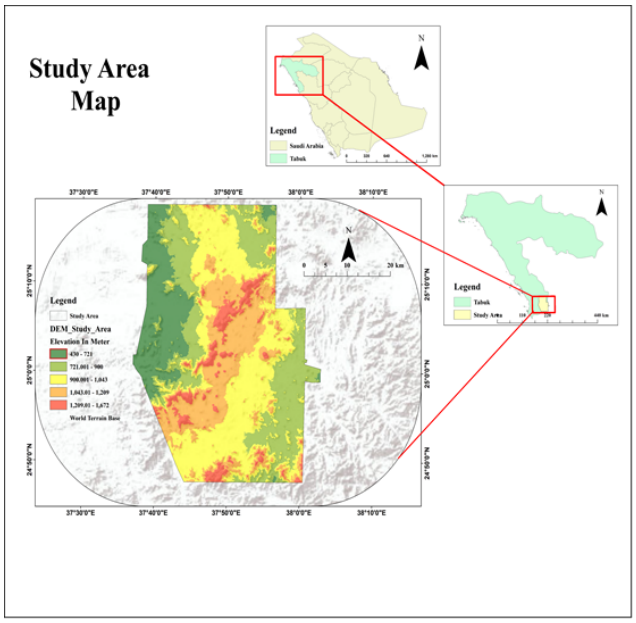

Figure 3. Study area map of Harrat Lunayyir, Saudi Arabia.

Stand-alone rocks from the Precambrian period form the eastern and northern as well as southern sections of Harrat Lunayyir. The middle section of the area consists of multiple rock strata but contains Precambrian rock formations in limited geological structures (**Figure 4**)[2]. The volcanic and seismic events within Harrat Lunayyir emerged around 0.5 million years ago. The most recent lava flow events could have taken place approximately 5000 years ago according to educated projections. The existence of a specific crater cone validates the possibility that volcanic eruptions occurred recently in this area according to Baer and Hamiel[11].

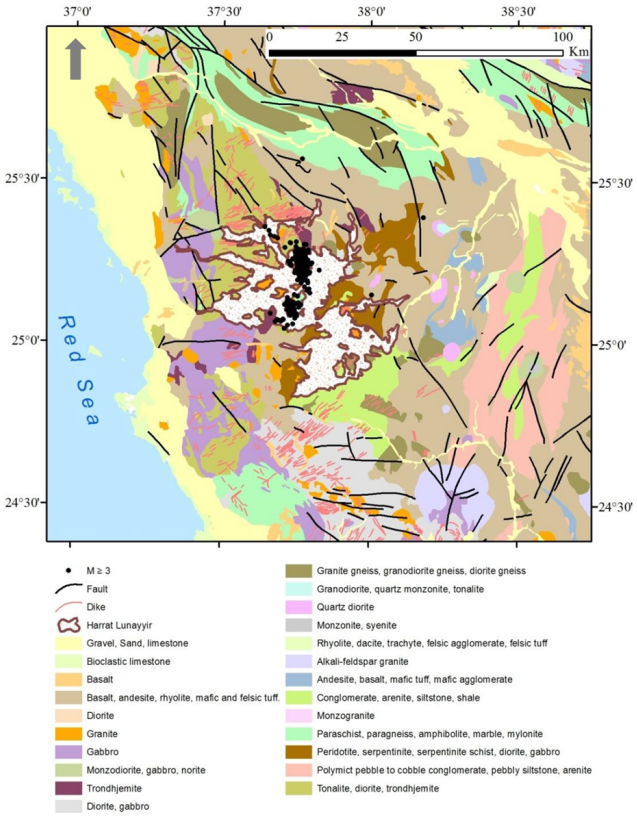

Figure 4. Geological setting around Harrat Lunayyir (modified from the work of Al-Zahrani et al.)[2].

2.1. Volcano Types in Harrat Lunayyir

Maars result from phreatomagmatic eruptions that are distinct from cinder cones, and lava flow fields are regions of solidified lava flows formed from effusive eruptions rather than explosive activity (**Figures 5** and **6**). The identification and classification of cinder cones in Harrat Lunayyir are based on a rigorous morphometric analysis of "crater characteristics (number of craters (Ncr))" and "cone morphology (cone major diameter (Wbco), cone minor diameter (WSco), cone elongation (Eco), crater major diameter (Wbcr), crater minor diameter (WScr), and crater elongation (Ecr))"[12]. As per this context, this study has categorized

these cones into four morphological types: "ring-shaped" (**Figure 5a**), "horseshoe-shaped" (**Figure 5d**), "multiple volcanoes" (**Figure 6a**) and "volcanoes without craters" (**Figure 6b**).

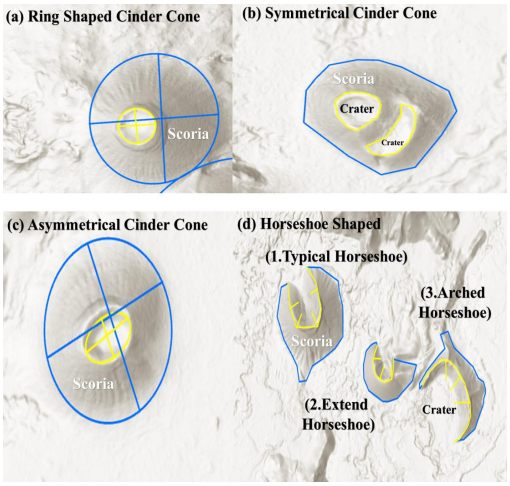

Figure 5. Morphological types of cinder cones in Harrat Lunayyir: (**a**) Ring-shaped (37.898ºE, 24.955ºN), (**b**) Symmetrical (37.77ºE, 25.282ºN), (**c**) Asymmetrical (37.910ºE, 25.083ºN), and (**d**) Horseshoe-shaped (37.910ºE, 25.083ºN).

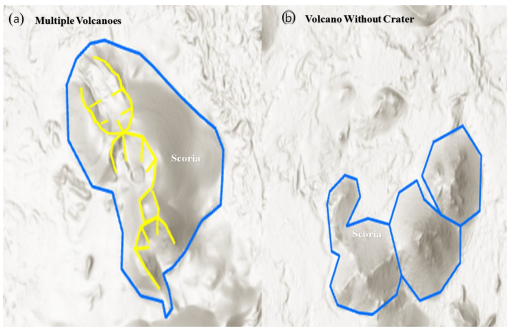

Figure 6. (**a**) Multiple volcanoes with more than one crater (37.78ºE, 25.21ºN). (**b**) Volcanoes without crater (37.990ºE, 25.033ºN).

2.1.1. Ring-Shaped Cinder Cones

Maars result from phreatomagmatic eruptions which are distinct from cinder cones and lava flow fields are regions of solidified lava flows formed from effusive eruptions rather than explosive activity (**Figures 5** and **6**). The identification and classification of cinder cones in Harrat Lunayyir are based on a rigorous morphometric analysis of "crater characteristics (Ncr)" and "cone morphology (Wbco, WSco, Eco, Wbcr, WScr, and Ecr)". As per this context, study has categorised these cones into four morphological types such as "ring-shaped", "horseshoe-shaped", "multiple volcanoes" and "volcanoes without craters".

2.1.2. Symmetrical Cinder Cones

Symmetrical cinder cones exhibit radial symmetry around their central vent by maintaining uniform slope angles, and they typically range between 15° and 30° (**Figure 5b**). Their overall shape is dependent on eruption dynamics and local geological conditions. The even distribution of lava flows and pyroclastic material results from the steady and continuous eruptions with a relatively uniform magma supply and gas content. Due to the impact of strong winds, cinder cones contribute to their distinct morphology by understanding monogenetic volcanic activity and landscape evolution.

2.1.3. Asymmetric Cinder Cones

Asymmetric cinder cones have an irregular shape with uneven slope angles which results from variations in eruption dynamics (**Figure 5c**). Their vents are commonly offset, leading to an asymmetrical structure. Lava flows and pyroclastic material are unevenly distributed due to the differences in magma composition and the prevailing winds as well.

2.1.4. Horseshoe-Shaped Volcanoes

Horseshoe-shaped volcanoes are a type of volcanic landform characterized by a curved or U-shaped configuration (**Figure 5d**). Result of sector collapse or flank failure, volcanic cone or edifice collapses due to gravity, magma withdrawal, or earthquakes debris avalanche and pyroclastic flows shape the horseshoe crater Curved or U-shaped crater Open end facing downhill or towards the ocean (if coastal) Steep inner walls and gentler outer slopes Volcanic cone or edifice remnants types.

- These volcanoes form due to the stratovolcano collapse along with caldera-like depression by remnants of the original cone
- Calderas are large and complex volcanic systems that result from the collapse of a magma chamber after a major eruption
- Horseshoe-shaped craters are associated with well-defined horseshoe-shaped craters along with the extended horseshoe and arched horseshoe as well.

2.1.5. Shield Volcanoes or Volcanoes without Craters

Shield volcanoes have a gently sloping shape resembling a shield, with a flat or rounded summit and no promi-

nent crater or caldera. They are typically formed by effusive eruptions. Lava flows are fluid and have low viscosity.

Formation:

- Shield volcanoes form due to the non-explosive eruptions that steadily release low-viscosity lava.
- Over time, lava flows build up and solidify by creating a broad sloping shield-like shape.
- The volcanic cone gradually increases in size, contributing to the overall growth of the volcano through the accumulation of successive lava flows.

3. Morphometric Analysis Methodology of Harrat Lunayyir

The research methodology in this paper depends on different qualitative and quantitative morphological parameters of the cinder cones (**Figure 7**). Morphological parameters were calculated using maps drawn at a 1:8,000 scale. The first category of these parameters includes the quantity, arrangement and geometric form of craters. Seven most effective quantitative metrics for shape definition serve as analysis tools for this study (Wbco, WSco, Eco, Ncr, Wbcr, WScr and Ecr)[3]. Seven morphological parameters let researchers examine the volcanic edifice with two elements limited to this specific structure (cone major and minor diameters and cone) (**Figure 8**).

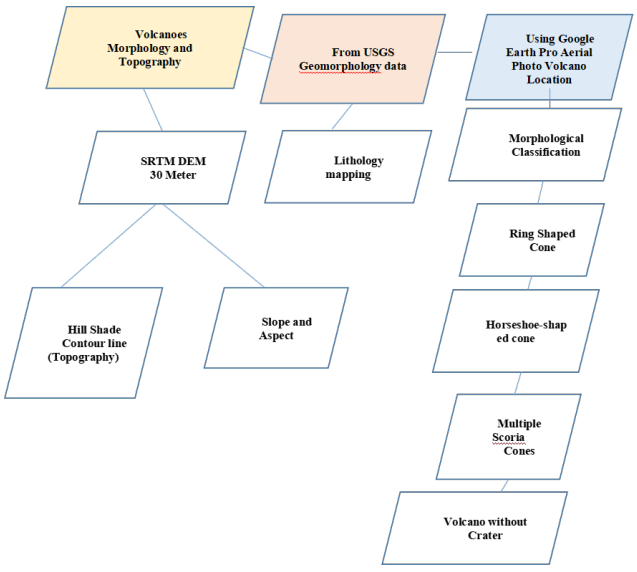

Figure 7. Flowchart of methodology for cinder cone classification using GIS, remote sensing, and morphometric analysis.

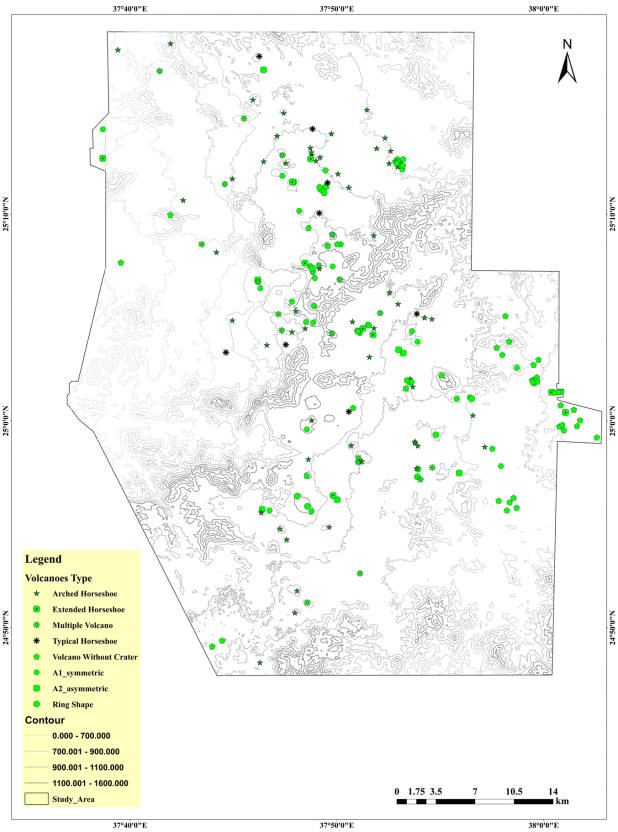

Figure 8. Topography of Harrat Lunayyir.

3.1. The Morphological Parameters Used in This Study

Aerial photography in conjunction with field research allowed scientists to properly identify crater regions. The analysis involves only crater identification since craters can house different volcanic vents. Wbco, WSco. The volcano is compared to either a circumference or an ellipse to find its parameters which are linked to the Wbco for the major axis and the WSco for the minor axis. Wbcr and WScr. Similar to cones, the shape of craters forms geometric figures which allows their major and minor diameters to be determined based on shape characteristics. The stretch of features in cones (Eco) matches the morphological distortion factor with the feature of craters (Ecr), revealing their morphological distortion factor (**Table 1**). These parameters measure the actual distance from the predicted circular perimeter. The Wbco and WSco calculate the ellipticity ratio and the Wbcr and WScr perform the same function (**Figures 9** and **10**)[13].

Table 1. Summary statistics of morphometric parameters for cinder cones in Harrat Lunayyir.

Morphometric Parameters	Average	Maximum	Minimum	Mean
Wb_{co}, Cone major diameter (m)	665.65875	1258.29	73.0275	488.863
WS_{co}, Cone minor diameter (m)	524.314	976.64	71.988	462.191
E_{co}, Cone elongation	2.1	6	1	0
N_{cr}, Number of craters	15	28	0	14
Wb_{cr}, Crater major diameter (m)	221.3645	414.768	27.961	169.709
WS_{cr}, Crater minor diameter (m)	137.5545	249.791	25.318	132.456
E_{cr}, Crater elongation	1.3	1.5	1	1.2

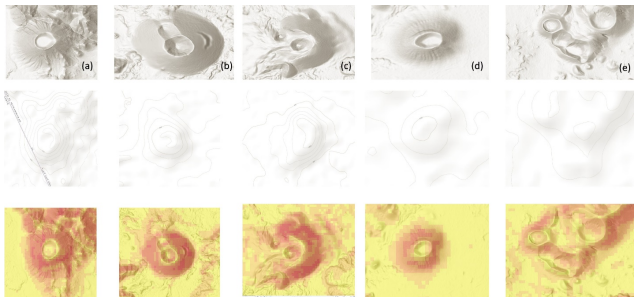

Figure 9. Geomorphometric maps of cinder cones: (**a**) Ring-shaped, (**b**) Extended horseshoe-shaped, (**c**) Arched horseshoe-shaped, (**d**) Asymmetrical, and (**e**) Typical horseshoe-shaped.

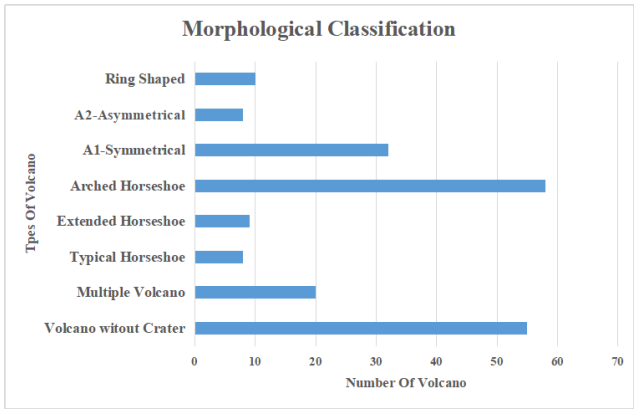

Figure 10. Morphological classification of cinder cones of Harrat Lunayyir.

The main facts are as follows (**Figures 11**, **12**, and **13**):

(1) The existence of cinder cones with (88.55% of cones) and without craters (11.45% of volcanoes) (N_{cr}).

(2) The existence of cinder cones with closed (13.13% of cones), open (69.02% of volcanoes) and open or closed craters (6.40% of cones) (geometry–morphology).

(3) The existence of volcanoes with very elongated plans and craters (E_{co} = N 1.6 and E_{co} = 1.6) and volcanoes with circular morphologies (E_{co} = ≤1.6).

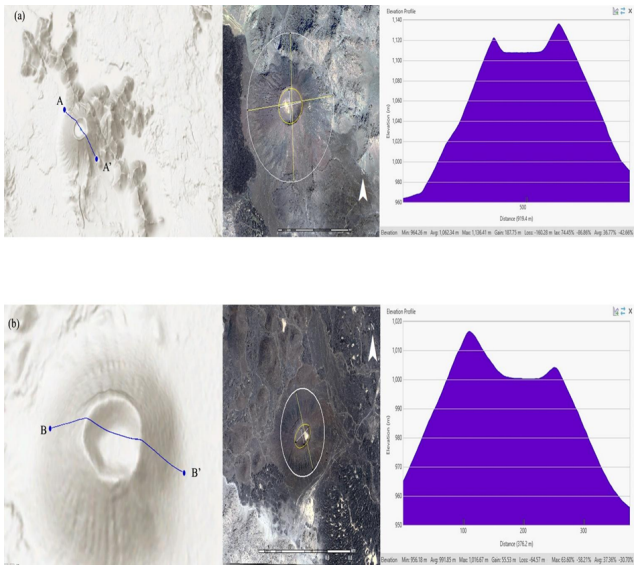

Figure 11. The profile of (**a**) ring cinder cone on the location latitude (37.913104), longitude (24.98881), and (**b**) asymmetrical cinder cone on the location of latitude (25.2829) and longitude (37.774) of Harrat Lunayyir.

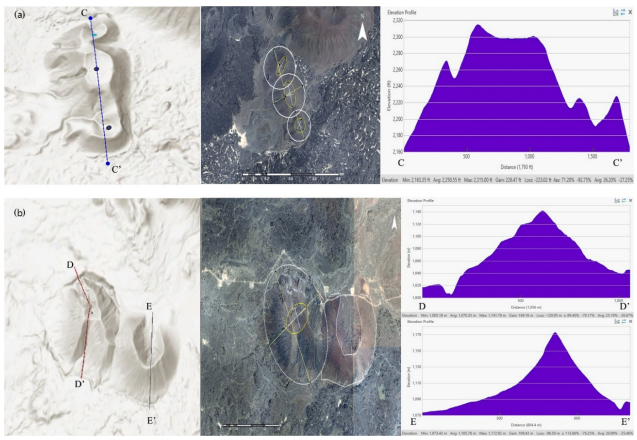

Figure 12. The profile of (**a**) multiple volcano on the location latitude (37.722) longitude (25.138) and (**b**) Typical Horseshoe-shaped volcano where profile line (D to D') while profile line (E to E') is arched horseshoe on location of latitude (25.072) longitude of (37.790) and latitude (25.072) longitude (37.797) of Harrat Lunayyir.

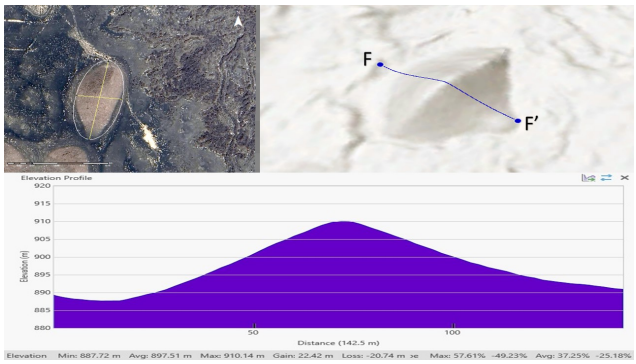

Figure 13. The profile of a volcano without a crater at the location latitude (37.885515), longitude (25.206667) of Harrat Lunayyir.

3.2. Lineament Density of Cinder Cones in Harrat Lunayyir

In cinder cone volcanic areas, high lineament density reflects intense fracturing and faulting, which is associated with increased volcanic activity and magma movement. This density also suggests potential hydrothermal activity and mineralization, as well as a complex geological structure and tectonic history. Fault zones and fracture networks provide pathways for magma and fluid flow, influencing volcanic conduit systems and dike networks. Additionally, these features may host hydrothermal veins and economic mineral deposits. High lineament density can also indicate geological instability, with potential risks of earthquakes and landslides (**Figure 14**).

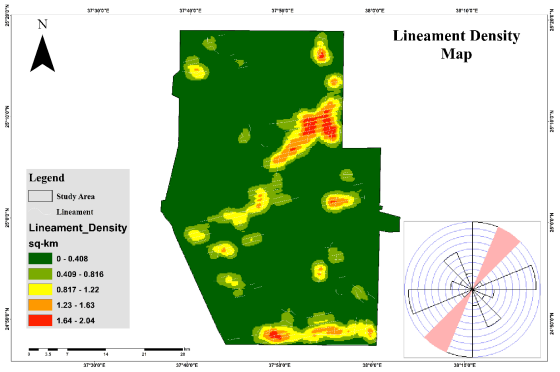

Figure 14. Lineament density map of Harrat Lunayyir, highlighting zones of high density (north to northeast) and moderate density (south to southeast). Spatial variations suggest preferential pathways for magma migration, which may influence lava flow distribution.

4. Result

In the study area, 200 volcanoes were identified, displaying variations in crater morphology and scoria composition. The following are a few representative examples.

4.1. Geomorphological Classification of Cinder Cones in Harrat Lunayyir

The analysis of the number, geometry and disposition of craters (Ncr) and the study of the morphometric parameters (Wb_{co}, WS_{co}, E_{co}, Wb_{cr}, WS_{cr} and E_{cr}) permit grouping of the cinder cones into four morphological types (**Table 2** and **Figure 15**).

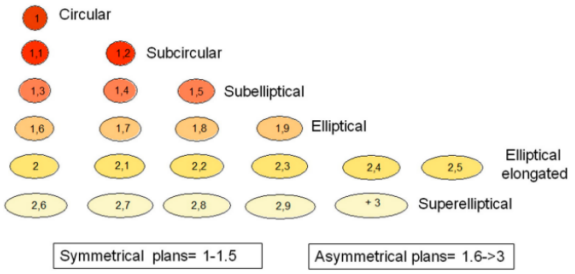

Figure 15. Plans of cinder cones: cone (E_{co}) and crater (E_{cr}) elongation (for interpretation of the references to color in this figure legend, the reader is referred to the web version of the article).

(A) Ring-shaped cones:

These cinder cones are characterized by circular or slightly elliptical shape (Eco = 1–1.6 and Ecr = ≤1.9) and closed craters. This category can be subdivided into two subgroups: Ring-shaped cones exhibit a "circular or slightly elliptical plan (Eco = 1–1.6)" with "enclosed craters (Ecr ≤ 1.9)" where cones are divided into "symmetrical and asymmetrical subtypes".

(B) A1_symmetric ring cones

"Symmetrical ring cones" display circular or subcircular shapes, such as "Eco ≤ 1.2, Ecr ≤ 1.2", along with "single crater (Ncr = 1)" for maintaining geometric regularity.

(C) A2_asymmetric ring cones

"Asymmetrical ring cones" present a slight elongation, such as "Eco ≤ 1.8, Ecr ≤ 1.6", which is marked as indicative of directional asymmetry. However, it is associated with "one or more craters (Ncr = 1–≥1)" by reflecting variations in volcanic activity or conduit geometry.

(D) Horseshoe-shaped volcanoes

Horseshoe-shaped cones exhibit open craters due to structural weaknesses or eruptive dynamics where classifications are determined based on the symmetry, crater shape, and slope variations.

(D1) Typical horseshoe-shaped cones

Table 2. Morphological classification of cinder cones in Harrat Lunayyir, grouped by elongation indices (E_{co}, E_{cr}) and crater number (N_{cr}).

Morphology of Cones	N° Cones	E_{cr}	E_{co}	N_{cr}
A1 symmetrical	32	1	1.1	1
A2 asymmetrical	8	1.6	2.7	1.2
Total ring-shaped cones	10	1.3	1.8	1.2
Typical horseshoe	8	1.8	1.1	1.3
Extended horseshoe	10	1.6	2.8	1.5
Arched horseshoe	61	1.5	1.4	1.19
Total horseshoe-shaped	79	1.6		1.9
Multiple volcanoes	38	1.3	1.2	1.5
Volcanoes without craters	68	-	6	-

"Typical Horseshoe-Shaped Cones" have a circular or slightly "sub-circular plan (Eco ≤ 1.2)" and one or more "open craters (Ecr = 1–≤1.9)".

(D2) Extended vertex ("tuning fork") horseshoe cones

"Extended Vertex ("Tuning Fork") Horseshoe Cones" are associated with the ways to develop elongated craters due to fissure-controlled eruptions or preexisting slopes. However, these plans indicate the tendency to be elliptical, along with multiple open craters contributing to irregular flank structures.

(E) Volcanoes without craters

A total of 200 volcanic hills within Harrat Lunayyir reveal horseshoe-shape volcanoes (N = 79) to be the most prevalent landform type with ring-shaped cones (N = 10) and multiple volcanoes (N = 38) and volcanoes without crater (N = 68) as fewer common features according to the morphological classification (**Table 2**). The two commonly identified volcanic styles which include horseshoe-shaped forms and ring-shaped cones represent 83% of the volcanic features in Harrat Lunayyir. These cones exhibit complex morphologies by containing either ring- or horseshoe-shaped structures with multiple craters "(N_{cr} = 2–10)". Their irregular formations arise from fissure eruptions, producing variable explosive activity and leading to crater coalescence and diverse edifice structures[14]. Their morphometry does not adhere to a uniform pattern which highlights the influence of dynamic eruption conditions.

Monogenetic volcanoes in Harrat Lunayyir result from fissure eruptions that shaped the rift zones but the eruptive activity does not persist evenly along the fissure zones hence separate individual volcanic morphologies came into being. According to Wood, Laki (Iceland) erupted from 1783 to 1785 and Timanfaya, while Lanzarote erupted from 1730 to 1736[9]. The total number of multiple cones in Harrat Lunayyir amounts to 28 despite this fact. These morphologically distinct volcanoes develop due to varied eruptive activities within this fracture system, thus preventing them from being classified as multiple edifices. The Fasnia volcano produced various cinder cones along a 1-km fracture that shows four distinct forms including ring-shaped cones and horseshoe-shaped volcanoes as well as multiple edifices and cones without craters.

These formations display symmetrical cone profiles ($E_{co} \leq 1.2$) and lack detectable craters due to erosion or burial under subsequent lava flows. Morphological analysis indicates that 28% of the volcanoes "(N = 55)" in Harrat Lunayyir fall into this category due to erosion masking their craters or volcanic material covering them[13]. Their presence in low-altitude areas suggests a strong link between topographic conditions and crater visibility.

4.1.1. The Ring- or Circular-Type Cinder Cones

Ring-type cones from Lunayyir present as very simple volcanoes, characterized by circular shapes with enclosed craters, as observed through morphological and morphometric analysis. This group of volcanoes consists of glacier-type cones that show circular shapes and homogeneous slopes along with symmetric cross-sectional profiles. The explosive patterns from specific parts of eruptive fissures become responsible for creating unique crater formations (A1-symmetrical ring-shaped) (**Figure 9**) or multiple coalesced vents of funnel morphology (A2-asymmetrical ring-shaped) (**Figure 9**) based on the fissure site explosive activity location. The essential craters stay circular and also display

gentle elliptical forms. Some ring-shaped cones generate lava flows through eruptive fissures that appear at the edges of their volcanic structures.

4.1.2. The Horseshoe-Shaped Volcanoes

A specific application of this classification bundles historical Canarian horseshoe volcanoes with Lanzarote volcanism (58)[15]. The three sub-types are arched, horseshoe-shaped volcanoes, with a 29% distribution, while typical and extended horseshoe each represent a 4% and 5% share, respectively. The land contains 38.0% arched horseshoe-shaped volcanoes which form the most prevalent volcanic features among basaltic monogenic volcanoes of Lunayyir while matching patterns found in other locations. Extended vertex horseshoe-shaped volcanoes stand as the least common morphological type according to current observations and also match the situation in Calatrava Volcanic Region (5%).

4.1.3. Multiple Volcanoes

A multiple volcano features either a ring-shaped volcano or an open, horseshoe-shaped cone structure, together with one or more craters that can be open or closed (**Figure 6**). The high Ncr results from complex explosive processes within eruptive fissures that form the final irregular shapes of flanks and plans and craters. The morphology of these volcanoes displays extensive irregularity since they do not match the regular structures of ring-shaped or horseshoe-shaped volcanoes. Multiple volcanoes acquire their diverse shapes through various controlling elements, including fissure features and dynamic eruption and slope surface characteristics.

4.1.4. Volcanoes Without Craters

Statistical justification for classification

The Arabian Plate experiences extensional forces that shape volcanic structures, which are influenced by the Red Sea rifting. The "Afar Triple Junction" has indicated that tectonic stress fields influence the formation of monogenetic volcanic fields. Similarly, Harrat Lunayyir has highlighted lineament density, which correlates with fault zones and structural weaknesses that guide magma ascent and cone alignment[16]. Moreover, this structural control is evident in other intraplate volcanic fields, such as those associated with Iceland and the Basin and Range Province in the western United States. The findings also contribute to the understanding of cinder cone longevity and degradation processes, as some volcanic cones in the study area lack craters (11.45%). This also raises questions about post-eruptive modification due to erosion, collapse, or burial by subsequent lava flows[17].

The morphometric classification of cinder cones is supported by statistical correlations between elongation indices (E_{co}, E_{cr}) and crater configurations (Ncr). **Table 3** summarizes the key relationships that demonstrate the symmetrical ring cones. Therefore, symmetrical ring cones exhibit minimal elongation variance "(E_{co} = 1.1–1.3, E_{cr} = 1.1–1.3)" where asymmetrical and horseshoe-shaped cones display higher elongation values "(E_{co} = 1.4–2.8, E_{cr} = 1.5–13)"[16]. The numerical distribution of volcano types aligns with prior findings by reinforcing the proposed classification's validity, along with indicating increased structural variability. The majority of the historical volcanic fields are associated with "Timanfaya and Laki," which has underscored the role of fissure eruptions in shaping volcanic morphology[17]. The predominance of horseshoe-shaped cones (38%) aligns with findings from other monogenetic volcanic provinces by substantiating the classification framework.

Table 3. Morphometric relationships between cone elongation (E_{co}), crater elongation (E_{cr}), and crater count (N_{cr}) for classified cinder cones.

Cinder Cone Type	N° Cones	Longitude	Latitude	E_{co}	E_{cr}	N_{cr}
A1_symmetric	1	37.80915	24.95556	2.8	2.9	0.2
A1_symmetric	1	37.81292	24.927209	1.5	6.8	0.2
A1_symmetric	1	37.89832	25.063888	0.9	1.8	0.3
A1_symmetric	1	37.82995	25.124457	2.4	5.6	0.1
A1_symmetric	1	37.81476	25.092575	1.7	4.2	0.1
A1_symmetric	1	37.78936	25.19757	1.9	3.7	0.1
A1_symmetric	1	37.81048	25.155364	1.5	3.7	0.1
A1_symmetric	1	37.85838	25.077601	3.1	3.7	0.2
A1_symmetric	1	37.9178	25.036576	1	3.7	0.1

Table 3. *Cont.*

Cinder Cone Type	N° Cones	Longitude	Latitude	E_{co}	E_{cr}	N_{cr}
A1_symmetric	1	37.92991	25.017764	1	3.7	0.1
A1_symmetric	1	37.81559	25.115108	3	3.7	0.1
A1_symmetric	1	37.81204	25.12475	2.8	1.8	0.2
A1_symmetric	1	37.64469	25.235038	1.2	5.6	0.1
A1_symmetric	1	37.79723	25.096087	2	4.2	0.1
A1_symmetric	1	37.77909	24.92788	2.3	4.4	0.1
A1_symmetric	1	37.80843	25.079694	2.3	4.2	0.1
A1_symmetric	1	37.96552	24.963574	2.1	3	0.3
A1_symmetric	1	37.82409	25.201868	2.8	3.2	0.1
A1_symmetric	1	37.7717	25.10691	1.4	3	0.2
A1_symmetric	1	37.76932	25.112287	9	3.1	0.1
A1_symmetric	1	37.81421	25.079118	2.1	4.4	0.2
A1_symmetric	1	37.81421	25.120281	2.3	4.1	0.1
A1_symmetric	1	37.82183	25.185487	2.7	2.1	0.1
A1_symmetric	1	37.79901	25.192529	1	2.2	0.2
A1_symmetric	1	37.94052	25.018914	2.3	2.1	0.1
A1_symmetric	1	37.97835	25.042854	2.3	2.5	0.1
A1_symmetric	1	37.80297	25.169271	2.1	2.5	0.1
A1_symmetric	1	37.85928	25.076891	2.1	2.4	0.1
A1_symmetric	1	37.85184	25.070825	2.3	3.1	0.1
A1_symmetric	1	37.89391	25.072359	2.7	2.5	0.3
A1_symmetric	1	37.8091	24.993219	2.3	2.8	0.1
A2_asymmetric	1	37.93188	24.957997	1.2	13	0.1
A2_asymmetric	1	37.83359	24.936444	1.9	10	0.1
A2_asymmetric	1	37.88682	25.0546	2.2	6	0.2
A2_asymmetric	1	37.88306	25.057351	4.5	4	0.2
A2_asymmetric	1	37.77422	25.28293	2.6	2	0.3
A2_asymmetric	1	37.76954	25.113652	3.2	3	0.1
A2_asymmetric	1	37.81348	25.122988	8.4	4	0.1
A2_asymmetric	1	37.77315	24.928685	3	8	0.2
Ring Shaped	1	37.82057	25.186358	5	4.7	0.2
Ring Shaped	1	37.82308	25.183745	13	7.4	0.1
Ring Shaped	1	37.94192	25.017855	4.3	8	0.3
Ring Shaped	1	37.9131	24.98881	1.1	7	0.2
Ring Shaped	1	37.80956	24.93113	1.7	9	0.1
Ring Shaped	1	37.80138	24.939355	8.3	8	0.2
Ring Shaped	1	37.89871	24.961145	6.3	6	0.1
Ring Shaped	1	37.89814	24.954958	3	12	0.2
Ring Shaped	1	37.82453	25.188638	3	5	0.1
Ring Shaped	1	37.81943	25.188138	1	5.1	0.1
Ring Shaped	1	37.7425	25.189879	8.6	15.8	0.2

E_{co} = Scoria Diameter x Cone elongation (Maximum height)
E_{cr} = Length of diameter x Crater elongation (Maximum height)
N_{cr} = Length of diameter x Crater elongation (Maximum height) x 1/slope of Crater

5. Discussion

Figure 16 presents two thematic maps of the Harrat Lunayyir volcanic field, illustrating spatial distribution and geological relationships. The left map shows the distribution and classification of volcanoes based on shape (e.g., symmetric, horseshoe, ring-shaped), with colour-coded contours indicating distance between volcanoes in metres. The right map visualises the distance between geological lineaments, also colour-coded by proximity. Both maps highlight the study area and use directional compasses and coordinate grids for orientation. The legends clarify volcanic types,

distances, and structural features, offering valuable insight into the region's volcanic and tectonic complexity for hazard assessment and geospatial analysis.

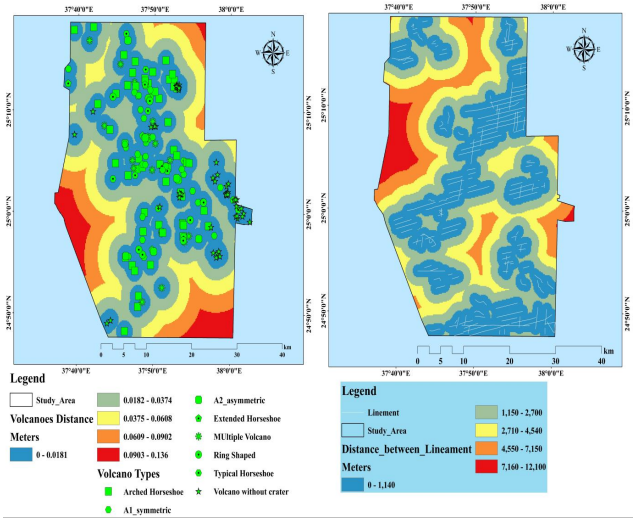

Figure 16. Distance between lineaments and volcanoes in the study area. Volcanoes without craters are located closest to lineaments, suggesting they may erupt in the future or develop craters.

The geological and geomorphological setting of Harrat Lunayyir provides an insightful basis for analyzing the classification of volcanic structures and their broader implications (**Figure 17**). This discussion compares the findings of this study with previous research by evaluating the methodology along with exploring the significance of classification approaches.

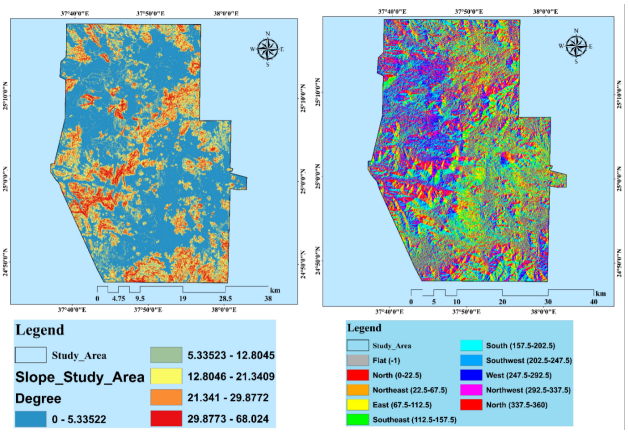

Figure 17. Slope and aspect analysis of Harrat Lunayyir.

A. Comparison with previous studies

The morphometric analysis of cinder cones in Harrat Lunayyir aligns with global studies on volcanic fields where it is focusing on monogenetic volcanic activity. Former literatures explain that Arabian Plate is associated with the rift systems where another former study has depicted that complex interplay of tectonic forces are responsible for shaping the region. The presence of both ring cinder cones and asymmetric cinder cones is consistent with findings in other intraplate volcanic fields where it has incorporated different sections through "San Francisco Volcanic Field in the United States"[18]. The study has differentiated existing perspectives in the proportions of volcano types and crater structures where 88.55% of cones contain craters along with the 11.45% lacking craters entirely. In contrast, studies of the Michoacán-Guanajuato volcanic field in Mexico indicate a higher prevalence of open craters[7]. These variations may be attributed to differences in magma composition along with analyzing the perspectives through eruption dynamics, and erosional processes.

The study's morphometric parameters suggest that Harrat Lunayyir exhibits a higher degree of elongation in cinder cones "(E_{co} = 2.1)" and it contrasts with the more symmetrical cones within the "Auvergne volcanic field" in France. This suggests regional structural controls by including faulting and stress orientations for developing a significant role in cone morphology[4]. The presence of open craters in 69.02% of studied volcanoes suggests significant variability in eruption styles which is compared to studies in the "East African Rift System"[19]. Harrat Lunayyir's cones demonstrate a more complex structural evolution which is influenced by the evolving rift dynamics of the Red Sea. Additionally, the high lineament density in the northern section of Harrat Lunayyir mirrors patterns have been observed in volcanic fields in Iceland and rift-related faulting influences cone alignment and elongation.

B. Differences in data, methodology, and findings

This study has incorporated high-resolution topographic maps (1:8,000 scale) alongside remote sensing and field observations. As per the comparison with the former predominantly on aerial photography, the integration of multiple data sources has improved accuracy in classifying volcanic structures[3]. Based on the statement, former studies have incorporated geochemical analysis and this research has focused primarily on geomorphological parameters. These clarifications and comparisons have limited insights into magma evolution and eruptive history through effective morphological classification. This former context has relied on

quantitative parameters such as "E_{co}" and "E_{cr}" effectively which characterizes the geomorphic diversity of volcanic cones[16]. However, previous research on cinder cones in the Arabian Shield has included the lava flow morphology and pyroclastic deposit thickness as the additional parameters. These parameters have provided further insights into volcanic activity where lack of detailed petrological data in this study presents a limitation[13]. However, these limitations have been put up by the variations in magma chemistry which could help explain observed morphological differences.

This context has included notable strength which has its emphasis on statistical analysis of cone shapes and crater configurations. This study has quantified traditional classifications which are associated solely on field observations and it is also related to the morphometric relationships by making it more reproducible[20]. However, future studies should integrate geophysical surveys to understand better subsurface structures along with its valid interpretations of volcanic formation processes.

C. Broader implications of the classification approach

The classification of volcanic structures in Harrat Lunayyir has important implications for understanding regional tectonics, hazard assessment, and planetary geology. The findings and former literature have incorporated variations in cone morphology which are influenced by both eruption dynamics and preexisting structural controls. These approaches are associated with the findings from Hawaiian volcanic fields where shield volcanoes are responsible for long-lived effusive eruptions and cinder cones result from short-lived explosive activity[8]. The presence of the monogenetic cones indicates the potential for future localised eruptions which has included the hazard assessment perspective. The predominance of open craters (69.02%) suggests that explosive eruptions are common and it has implications for risk management in the region[15]. Similar classifications have also depicted that "Chichinautzin volcanic field in Mexico" have shown new cinder cones which can indicate the unexpected risks to nearby populations. Moreover, these classifications have been presented in this study to provide a valuable tool for monitoring potential future eruptions.

The findings also have implications for planetary geology where Volcanic fields on Mars, "Elysium Planitia", have exhibited similar morphometric characteristics within the Harrat Lunayyir[14]. Based on the former literature, researchers can improve interpretations of extraterrestrial volcanic landscapes.

D. Discussion on the influencing factors

The high lineament density in the northern region suggests that tectonic controls have played a key role in cone orientation and morphology. Therefore, similar findings have been observed in the East African Rift where stress fields influence cone alignment. Magma composition in cinder cone morphology could be linked to differences in magma viscosity and volatile content. It is associated with the "High-alkaline basalts" where Arabian volcanic fields tend to produce more fluid lava flows by influencing cone structure[10]. It is also suitable for analysing the erosion process where the asymmetry has been observed influencing cone structure. Moreover, this scenario has incorporated wind erosion and gravitational collapse which might modify the original volcanic forms[11]. Majority of the former studies have included the arid environments which is indicating the wind direction and the wind direction has already significantly impacted cone degradation.

E. Future research directions

Geographic analysis has conducted detailed geochemical studies of lava flows and pyroclastic deposits which would help clarify the magmatic evolution of Harrat Lunayyir. Geophysical surveys have employed ground-penetrating radar and seismic imaging which can reveal subsurface structures through the process of improving the understanding of volcanic conduit systems. Based on the clarifications, long-term monitoring has established a volcanic hazard monitoring system which has included satellite-based thermal imaging through assessing ongoing activity in the region[13]. Based on the clarifications, comparative planetary studies have utilised the data from Martian volcanic fields to refine classification approaches and improve interpretations of extraterrestrial monogenetic volcanoes. Based on the clarifications, numerical modelling has developed models to simulate cinder cone formation under varying tectonic and eruptive conditions which can enhance predictive capabilities for future volcanic activity.

6. Conclusions

This paper presents a morphological classification system for the basaltic monogenetic volcanoes within Harrat

Lunayir which uses combined quantitative and qualitative assessments of volcano cone features. Among the qualitative features used for classification are the crater numbers along with their geometrical shape and spatial arrangement. The classification employs measurement parameters consisting of Wbco and WSco along with Eco and Ncr and Wbcr and WScr and Ecr. The three main volcanic landform classification methods in volcanic geomorphology consist of dynamic systematizations and morphological method along with their combination. A mainly morphological classification scheme is established yet elements from eruptive dynamics and behavior also enter into consideration. Among all Lunayyir volcanoes, the two traditional open horseshoe-shaped and ring-shaped monogenic basaltic forms create a very high occurrence reaching 82% while pyroclastic mountains constitute 19% and multiple volcanic edifices account for 6%.

The mutual relationship between the volcanic locations and their topographic characteristics and eventual volcanic shape exists in a positive manner. The low morphometric indexes of ring-shaped volcanoes as well as pyroclastic mountains occur because these eruptions develop at gentle slopes (N25°) between features of small height difference. Conversely, higher morphometric indexes exist at locations where open horseshoe-shaped volcanoes and multiple edifices form because these have more complex morphologies.

The combination of monogenetic volcanism technique helps locate volcano morphologies and geological spatial mapping using hill shade and lineament density shows future potential lava emergence sites through geo spatial data collection that this approach works on any land formation globally.

Funding

This work received no external funding.

Data Availability Statement

The data utilized in this study was obtained from publicly available sources on the internet. The specific websites and platforms from which the data was collected have been appropriately cited and acknowledged within the manuscript.

Acknowledgments

This manuscript is authored by a single author.

Conflicts of Interest

The author declares no conflict of interest.

References

[1] Al-Amri, A., Fnais, M., Abdel-Rahman, M., et al., 2012. Geochronological dating and stratigraphic sequences of Harrat Lunayyir, NW Saudi Arabia. International Journal of Physical Sciences. 7, 2791–2805. DOI: https://doi.org/10.5897/IJPS12.178

[2] Al-Zahrani, N., Baron, D., Sabourin, A., 2013. Ste20-like kinase SLK, at the crossroads: a matter of life and death. Cell Adhesion & Migration. 7(1), 1–10. DOI: https://doi.org/10.4161/cam.22495

[3] Kervyn, M., Ernst, G., Goossens, R., et al., 2008. Mapping volcano topography with remote sensing: ASTER vs. SRTM. International Journal of Remote Sensing. 29(22), 6515–6538. DOI: https://doi.org/10.1080/01431160802167949

[4] Criado, A., 1984. Lattice dynamics and thermal crystallographic parameters in phenothiazine. Acta Crystallographica Section A: Foundations and Advances. 40(6), 696–701. DOI: https://doi.org/10.1107/S0108767384001422

[5] Omar, G., Steckler, M., 1995. Fission track evidence on the initial rifting of the Red Sea: Two pulses, no propagation. Science. 270(5240), 1341–1344. DOI: https://doi.org/10.1126/science.270.5240.134

[6] Dehn, J., 2002. Thermal precursors in satellite images of the 1999 eruption of Shishaldin Volcano. Springer natuew link. 64, 525–534.

[7] Corazzato, C., Tibaldi, A., 2006. Fracture control on type, morphology and distribution of parasitic volcanic cones: an example from Mt. Etna Italy. Journal of Volcanology and Geothermal Research. 158, 177–194. DOI: https://doi.org/10.1016/j.jvolgeores.2006.04.018

[8] Thordarson, T., Self, S., 1993. The Laki (Skaftár Fires) and Grímsvötn eruptions in 1783–1785. Bulletin of Volcanology. 55, 233–263. DOI: https://doi.org/10.1007/BF00624353

[9] Wood, C.A., 1980. Morphometric evolution of cinder cones. Journal of Volcanology and Geothermal Research. 7(3–4), 387–413. DOI: https://doi.org/10.1016/0377-0273(80)90040-2

[10] Bonatti, P., Colantoni, B., Della, V., et al., 1984. Geology of the Red Sea transitional zone (22°N–25°N). Oceanologica Acta. 7(4), 385–398.

[11] Baer, G., Hamiel, Y., 2010. Form and growth of an embryonic continental rift: InSAR observations and modelling of the 2009 western Arabia rifting episode. Geophysical Journal International. 182, 155–167. DOI: https://doi.org/10.1111/j.1365-246X.2010.04627.x

[12] Stern, R., Johnson, P., 2010. Continental lithosphere

of the Arabian Plate; a geologic, petrologic, and geophysical synthesis. Earth-Science Reviews. 101, 29–67. DOI: https://doi.org/10.1016/j.earscirev.2010.01.002

[13] Manville, V., Németh, K., Kano, K., 2009. Source to sink: a review of three decades of progress in the understanding of volcaniclastic processes, deposits, and hazards. Sedimentary Geology. 220(3–4), 136–161. DOI: https://doi.org/10.1016/j.sedgeo.2009.04.022

[14] Romero, R., Carrasco, D., Araña, V., et al., 2003. A new approach to the monitoring of deformation on Lanzarote (Canary Islands): an 8-year radar perspective. Bulletin of Volcanology. 65, 1–7. DOI: https://doi.org/10.1007/s00445-002-0232-3

[15] Stoeser, D., Camp, E., 1985. Pan-African microplate accretion of the Arabian Shield. Geological Society of America Bulletin. 96(7), 817–826.

[16] Le Corvec, N., Spörli, B., Rowland, J., et al., 2013. Spatial distribution and alignments of volcanic centers: clues to the formation of monogenetic volcanic fields. Earth-Science Reviews. 124, 96–114. DOI: https://doi.org/10.1016/j.earscirev.2013.05.005

[17] Riedel, C., 2003. Controls on the growth and geometry of pyroclastic constructs. Journal of Volcanology and Geothermal Research. 127(1–2), 121–152. DOI: https://doi.org/10.1016/S0377-0273(03)00196-3

[18] Porter, C., 1972. Distribution, Morphology, and Size Frequency of Cinder Cones on Mauna Kea Volcano, Hawaii. Geological Society of America Bulletin. 83, 3607–3612.

[19] Doniz Paez, F.J., 2004. Caracterización geomorfológica del volcanismo basáltico monogénico de la isla de Tenerife [Doctoral dissertation]. Universidad de La Laguna: La Laguna, Spain.

[20] Thouret, J.-C., 1999. Volcanic geomorphology—an overview. Earth Science Reviews. 47, 95–131. DOI: https://doi.org/10.1016/S0012-8252(99)00014-8